Fusion Engineering and Design 18 (1991) 397–405
North-Holland

Direct nuclear heating measurements in fusion neutron environment and analysis

A. Kumar, M.Z. Youssef, M.A. Abdou

School of Engineering and Applied Science, University of California at Los Angeles (UCLA), Los Angeles, CA 90024, USA

Y. Ikeda, C. Konno, K. Kosako, Y. Oyama, T. Nakamura

Department of Reactor Engineering, Japan Atomic Energy Research Institute, Tokai, Ibaraki 319-11, Japan

Experimental measurement of nuclear heating rates has been carried out in a simulated D–T fusion neutron environment from 1989 through 1990 under the USDOE/JAERI collaborative program at the Fusion Neutronics Source Facility. The microcalorimetric technique has been employed for online measurements. Small probes of materials have been irradiated in close vicinity of a rotating target. A typical probe contains a core measuring 2 cm in diameter by 2 cm in length. Probes of leading candidates, for different applications, have been investigated: molybdenum, tungsten, titanium, graphite (plasma facing components), copper (magnet coils), iron, stainless steel 304, nickel (structural material components) and aluminum. The measured temperature-change rates range from 30 μK/s (iron) to 330 μK/s (graphite). The corresponding nuclear heating rates range from ~ 35 μW/g (tungsten) to ~ 225 μW/g (graphite). These measurements have been analyzed using three dimensional Monte Carlo code MCNP and various heating number/kerma factor libraries. The ratio of computed to measured heating rates shows large deviation from 1 for all the materials. In addition, there is a large spread for different libraries; for example, this ratio varies from 1.03 to 1.81 for aluminum. Also, there have been three experiments with each having a host medium of iron, graphite or copper, that measures 85 mm in diameter by 100 mm in length. Small single probes of the host medium graphite and tungsten are placed inside to measure the spatial profile of heat deposition. Analysis of the measurements shows that the ratio of computed to measured rates varies widely, e.g., in iron host, it goes from 0.5 to 1.1. Further effort is to be invested to locate the sources of this discrepancy.

1. Introduction

Experimental measurement of nuclear heat deposition rates in a simulated D–T fusion neutron environment has been carried out over last two years [1,2] to create a data base for validating kerma factor/heating number libraries [3–11]. These data bases are largely untested and have been playing a crucial role in the design and related aspects of leading fusion devices, e.g., ITER, CIT, NET, FER. The results of these measurements will be helpful in arriving at crucial decisions concerning the selection of materials for fusion device components as the related parameters, e.g., thermal laod bearing capacity and maximum attainable temperature, play important roles there.

An experimental effort was initiated in 1988 to develop and apply the microcalorimetric technique to measure heat deposition in various materials subjected to D–T neutron fields, in the framework of the JAERI/USDOE collaborative program on fusion neutronics [1,2]. Materials, in contention as leading candidates for various applications, i.e., molybdenum, tungsten, titanium, graphite (plasma facing components), copper (magnet coils), iron, stainless steel, nickel (structural material components), aluminum, etc., were targeted for experiments. Bead thermistors and platinum resistance temperature detectors were employed as thermal sensors within calorimeters made of single materials (or probes). The first experiments were conducted during June 1989 and the tested materials included: Fe, Al, C, Cu. Each of these calorimeters was placed inside a vacuum chamber and the mean distance from the target was ~ 8 cm. Experiments were also conducted on an iron probe without vacuum chamber. The calorimeters were subjected to spaced neutron pulses of 3 to 10 min duration. The measured heat deposition rates ranged from 7 to 30 μW/g for a normalized source strength of 10^{12} n/s, iron and graphite providing the lowest and the highest rates, respectively. The single probe experiments were car-

ried out again in December 1989. This allowed to verify the reproducibility. This time, the average target–probe distance was shortened to ~ 5 cm which led to 2 to 3 times higher rates. Tungsten was also included. In addition to single probe experiments, two novel experiments were conducted with multiple probes in separate host media of iron and graphite. Most recently, during November 1990, experimental measurements were conducted on small single probes of graphite, titanium, stainless steel 304, nickel, molybdenum and tungsten. In addition, the multiple probe experiment was extended to copper.

2. Experiments

The microcalorimetric technique has earlier been applied for neutron/gamma dosimetry [12–16] and nuclear heat deposition rate measurements in fission reactors [17–19]. However, the application of this technique to measure the nuclear heat deposition rate with currently available D–T neutron sources, maximum source strength being $\sim 10^{12}$ n/s, requires careful experimentation owing to significant noise from the ambient temperature fluctuations [1].

Nuclear heating measurements using the microcalorimetric technique were conducted in June 1989, December 1989 and November 1990 at the Fusion Neutronics Source facility (FNS) of JAERI. A rotating neutron target (RNT) source, having a nominal intensity of $\sim 3 \times 10^{12}$ n/s, was selected for obtaining larger heat deposition rates [1,2]. Bead (point-size) thermistors (TM) and platinum resistance temperature detectors (RTD) were employed as thermal sensors. Four types of thermistors were employed, having 25 °C resistances of 2.252 KΩ, 10 KΩ, 22 KΩ, and 30 KΩ. The 2.252 KΩ and 30 KΩ thermistors were obtained from the Omega Engineering Corporation and 10 KΩ and 22 KΩ thermistors came from the Alpha Thermistor Company. A platinum RTD had a resistance of 100 Ω at 0 °C. The temperature coefficient of resistance for a thermistor and a platinum RTD were -4.4×10^{-2} per °C (at 25 °C) and $+3.6 \times 10^{-3}$ per °C (at 0 °C), respectively.

2.1. Instrumentation

The very small temperature changes produced with currently available fusion neutron sources demand high precision and sophisticated instrumentation, in addition to highly sensitive and stable thermal sensors, for reliability and reproducibility. The temperature changes of interest could be as low as 1 μK/s for heat deposition rates in the range of 1 μW/g [1,2]. All these considerations led to adoption of the following strategy [1,2]:

(1) Instrumentation to be based on usage of IEEE-488 bus based equipment.

(2) Perform measurements on small size probes, preferably a 20 mm diameter × 20 mm long core, either alone or enclosed within a 1 mm thick jacket measuring 32 mm diameter × 32 mm long; a small probe will enable quick equilibration of nuclear heat generated in the probe.

(3) Isolate the probe from the surroundings by keeping it inside an evacuated vacuum chamber.

(4) The neutron source will be pulsed so as to have 3 to 10 min duration spaced pulses; the source intensity will be flat during a given pulse; the probe will be kept as close to the target as possible.

(5) Measure periodically, with a pre-determined cycle length (20 to 30 s), the resistance of a thermal sensor, thermistor (TM)/platinum RTD, using a highly sensitive nanovoltmeter or a high-resolution digital multimeter.

(6) Study the resistance change per cycle over the entire irradiation history and obtain its component directly assignable to the source neutron induced heat deposition.

The system configuration for picking up low level voltage changes developing on a thermal sensor, kept in direct thermal contact with a probe, is shown in fig. 1. The controller was PC based: HP3497A or Macintosh SE (supplemented by a MacSCSI/IOtech interface and MacDriver488 driver software). While using the Macintosh SE, the programmable current source of the HP3497A was used as such. Two scanners (model 705, Keithley) were used to separately switch TMs and RTDs. For TM switching the model 7168 nV scanner card of Keithley was used. A single card can take up to 8 TMs. 10 μA was passed through a TM to measure its voltage output by a nanovoltmeter with a resolution of 10 nV in the 2 mV range. 1 mA was passed through a RTD to measure its output by a Model 7081 precision voltmeter of Solatron. Also a ratemeter was included to broadly monitor the source neutron pulse history during an irradiation. The data acquisition process was driven by a BASIC program residing on the controller.

2.2. Single probe experiments

There have been concerns regarding fast neutron induced damage adversely affecting the performance of a thermistor. This was addressed before proceeding

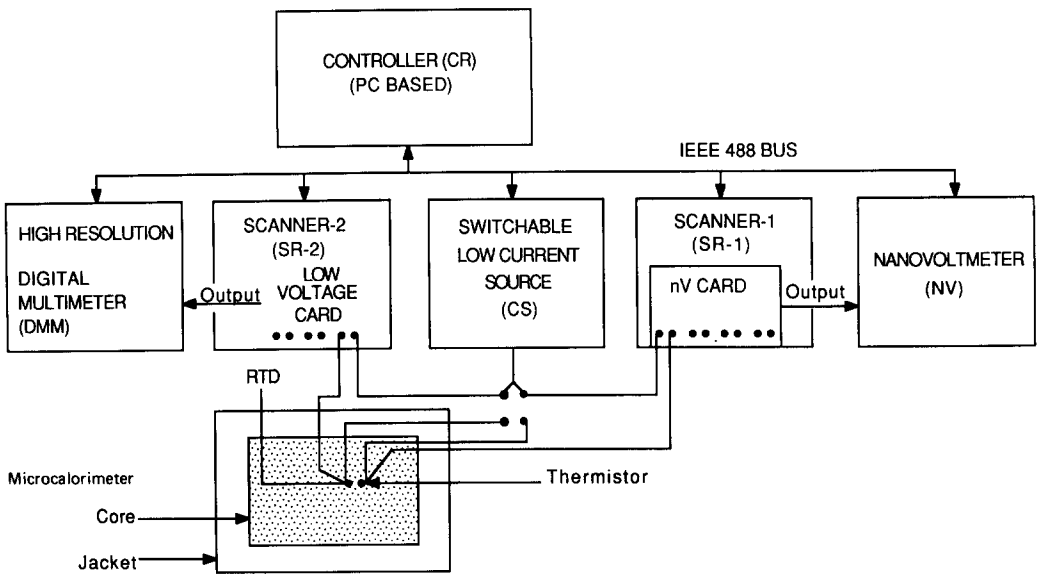

Fig. 1. System configuration for low voltage measurements.

with thermistor use in the first experiments done during June 1989 [1]. It was experimentally demonstrated that there was a negligible likelihood of a thermistor suffering any degradation as long as the neutron fluence was below 10^{14} n/cm^2, a safe limit for measurements to follow [1].

Single probe experiments have been conducted during June 1989, December 1989 and November 1990. Figure 2 shows a schematic of the single probe experiments conducted in June and December 1989. Table 1 lists important details about these experiments. A typical probe consists of a core, measuring 20 mm in diameter by 20 mm in length, that sits symmetrically inside a 1 mm thick jacket, with external diameter and height of 32 mm each. During December 1989, a single tungsten probe, measuring 1 in. across with a vertical cross section of 2 in. × 2 in., was also included. The experiments done in November 1990 had all probes without jacket. Typically, a probe measured 2 cm in length × 2 cm in diameter. Each probe was placed inside an evacuated vacuum chamber that measured 15 cm in length × 10 cm in diameter. The vacuum chamber had an only 1 mm thick front wall.

During the June and December 1989 experimental periods, thermal sensors were placed as follows: thermistors on the front and back flat surfaces of the core

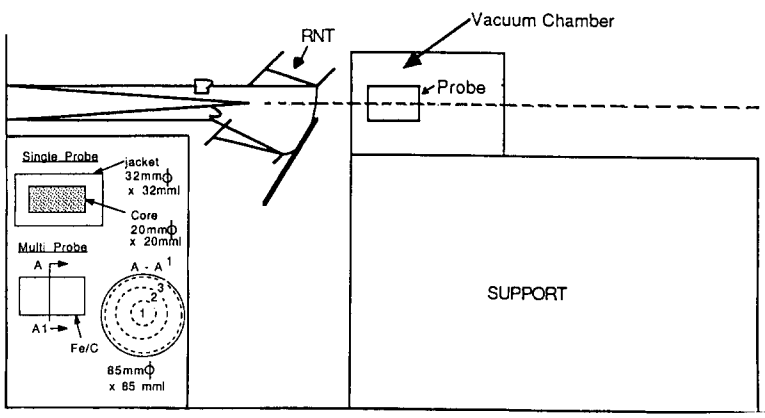

Fig. 2. Schematic arrangement for nuclear heating experiments.

plus close to its center: two RTDs, such that one was located, vertically to the axis of symmetry of the core, in the middle of the first half and the other one was placed in the middle of the latter half of the core. In the case of tungsten, a "10 KΩ" thermistor was placed at the center of the front surface and another thermistor of the same type was placed at the center of its back surface. Three additional thermistors and two RTDs were used for measurements outside the probes: (i) a 2.252 KΩ thermistor and a RTD were located on the target surface close to the source neutron generation area to follow the source temperature variation during the course of each experiment, (ii) a 2.252 KΩ thermistor and a RTD were more than a meter away from the target to observe ambient temperature fluctuations, (iii) a 2.252 KΩ thermistor was located on the inside of the front wall of the vacuum chamber. Apart from these additional sensors, three Nb foils were used in each experiment to monitor the source neutron flux across the probe. A Nb foil was located on the center of the front surface of the probe another Nb foil was attached to the back surface. A third Nb foil was attached to the outer surface of the front wall of the vacuum chamber. During the November 1990 experimental period, only two niobium foils were used per probe: one in front and the other behind a probe to obtain the drop in ^{92m}Nb activity across it. Each probe was kept in a vacuum chamber measuring 15 cm in length by 10 cm in diameter.

2.3. Multiple probe experiments

Three host media made individually of iron, graphite (during December 1989), and copper (during November 1990) were impregnated by single probes of W, C, and Fe/Cu. Each host medium measured 85 mm diameter × 100 mm long and had multiple holes, each measuring 5 mm diameter × 16 mm long to house 10 mm long probes. No probe was allowed to have direct thermal contact with the host medium. The front surface of the host medium was at 38 mm from the target for ion and graphite and it was at 36 mm for copper. A thermistor was attached to each of these probes. Probes made of the material of the host medium were located in the first and second halves to measure axial and radial profiles of the total nuclear heat deposition rates in the host. Probes of W and C (graphite) were introduced in the second half to largely measure the gamma and neutron components of the total nuclear heat

Table 1
Characteristics of single probe experiments

Probe material	Experimental period	Target-core distance [a] (cm)	Irradiation pulses' duration	Comments
C	June 1989	7.9	10m	
	December 1989	4.4	3m/5m/11m	
	November 1990	3.6	5m	w/o jacket
Al	June 1989	7.8	3m/10m/30m	
	December 1989	4.4	3m/5m	
Ti	November 1990	3.6	5m	w/o jacket
Fe	June 1989	8.3	3m/10m/11m	
	December 1989	4.4	3m/5m/35m	
SS304	November 1990	3.6	5m	w/o jacket
Cu	June 1989	7.8	10m	
	December 1989	4.4	3m/5m	
Ni	November 1990	3.6	3m/5m	w/o jacket
Mo	November 1990	3.6	5m	w/o jacket
W	December 1989	4.4	3m/5m	w/o jacket
	November 1990	3.6	5m	w/o jacket

[a] Distance measured from front flat surface of a core of a probe.

deposition radial profile, respectively. They were placed on three concentric surfaces with radii of 10, 20 and 30 mm. By applying cavity theory [20], both the components of the nuclear heat deposition rates could be extracted, in principle.

3. Analysis

The three-dimensional code MCNP [21] was used for modeling the RNT geometry and the probe–vacuum chamber system. The background contribution is found negligible due to the close proximity of the probe to the neutron source and hence it was subsequently ignored in all the computations. The RMCCS library was used for neutron interactions and photon production in the whole system. This library has many cross-sections based on ENDF/B-V. The particle transport computations were repeated with the ENDL85 library and an insignificant difference was seen between the neutron/photon fluxes evaluated by the two libraries. Heating numbers from the four libraries available [21] with MCNP, i.e., BMCCS, ENDL85, RMCCS, ENDF5T (or ENDF5U), were used for a comparison of nuclear heating rates. It is to be noted that ENDF5T/ENDF5U, and RMCCS, to large extent, have data obtained from ENDF/B-V; ENDL85 is the latest library from the Lawrence Livermore National Laboratory; BMCCS contains older data, i.e., from ENDF/B-IV or ENDL73 files. In addition, KAOSLIB [5], a new kerma factor library generated from the ENDF/B-V library using KAOS-V code [5], was used with the neutron flux obtained from MCNP to get neutron heating rates for all materials. RMCCS, ENDF5T/ENDF5U, and BMCCS (if from ENDF/B-IV) libraries contain heating numbers obtained by the "direct energy balance" method [5,10,11,22]. MCNP provides for ignoring negative contributions [22–24], if any. ENDL85 has positive heating numbers that are used to adjust photon production cross-sections and spectra for self-consistency [5,9,22]. MCPLIB was utilized for photon interactions and transport. The heat deposition rate drops very rapidly across the core due to its proximity to the source. However, since the experimental conditions are designed to lead to quick thermal diffusion across the core of an isolated probe, the heat deposition rate has to be averaged over the entire core to obtain the quantity that is to be compared to experimental measurements. The nuclear heat deposition rate, expressed in μW/g, is converted to the temperature-change rate, expressed in μK/s, using specific heat data from ref. [25].

4. Results and discussion

4.1. Experimental data

Figures 3a through 3f show the typical resistance change per cycle (length = 20 s) as a function of cycle no. for a TM or RTD placed inside single probes of graphite, titanium, stainless steel 304, nickel, molybdenum and tungsten in experiments during November 1990. These figures also show the relative "14 MeV" neutron intensity as measured by the ratemeter. It is to be noted that the onset of the neutron source leads to an instantaneous drop in the resistance of a TM that shows up as a dip in the drift curve. On the other hand, an RTD in such a situation shows an instantaneous raise in its resistance. Abrupt and large changes seen in the curves for graphite (fig. 3a) and molybdenum (fig. 3e) are due to stray electromagnetic signals. Figure 4 shows a typical temporal profile of the resistance change per cycle (length = 30 s) for an RTD embedded radially on the mid-plane in copper host. This RTD is in direct thermal contact with the host medium and, thus, measures the average nuclear heat deposited therein. Niobium foils, placed in front and back of each probe, were counted for monitoring the drop in the ^{93}Nb(n, 2n)^{92m}Nb reaction rate across it. This drop is expected to be a good index of the correctness of the positioning of a probe vis-a-vis the target. The uncertainty in the measured reaction rates varies from 3 to 6%.

Figure 5 shows the nuclear heating rates, expressed in units of μK/s for a normalizing source intensity of 10^{12} n/s, for single probes of C, Ti, SS304 (or SS), Ni, Mo, W of the November 1990 experimental period and for Al, Fe and Cu of the December 1989 period. In what follows, only these single probes will be touched upon. It is to be underlined here that one is looking here (fig. 5) at the temperature change rate only. The lowest value is seen for Ti and the highest for C. In fact, if the temperature change rate is converted to obtain the heat deposition rate, expressed in units of μW/g, C tops with a value of ~ 90 μW/g and W yields the lowest rate of ~ 12 μW/g. Taking the actual source neutron intensity into account for each probe, the heat deposition rates range from ~ 35 μW/g (tungsten) to ~ 225 μW/g (graphite), whereas the corresponding temperature change ranged from ~ 103 μK/s (titanium) to ~ 325 μK/s (graphite). However, temperature rates as low as ~ 30 μK/s were already measured in the iron and copper probes during the June 1989 experiments [1,2].

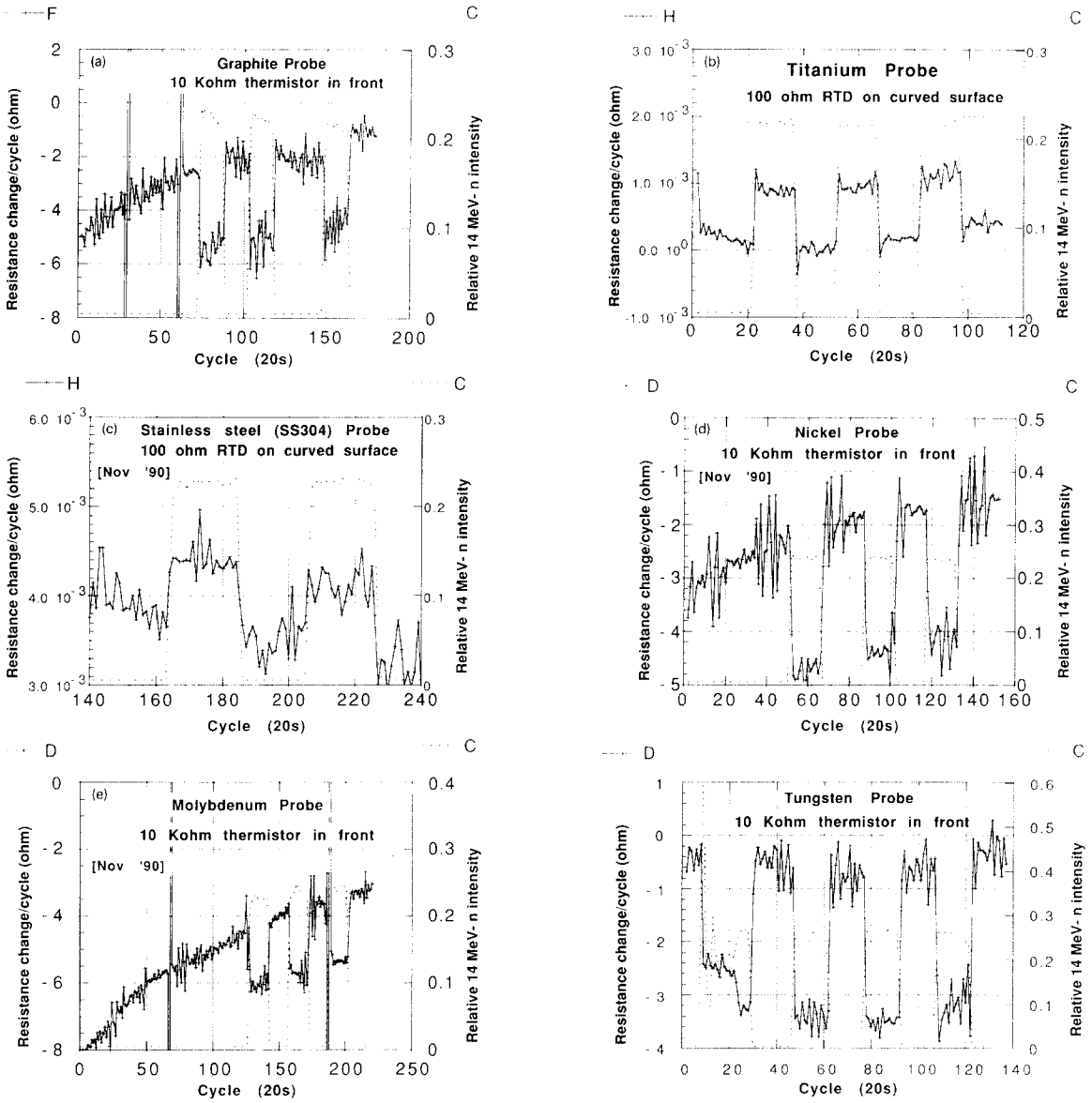

Fig. 3. (a) Graphite probe (November 1990): Temporal profile of the temperature change rate observed via a 10 KΩ thermistor kept in front. (b) Titanium probe (November 1990): Temporal profile of the temperature change rate observed via a 100 Ω platinum RTD kept on curved surface along axis. (c) Stainless steel SS304 probe (November 1990): Temporal profile of the temperature change rate observed via a 100Ω platinum RTD kept on curved surface along axis. (d) Nickel probe (November 1990): Temporal profile of the temperature change rate observed via a 10 KΩ thermistor kept in front. (e) Molybdenum probe (November 1990): Temporal profile of the temperature change rate observed via a 10 KΩ thermistor kept in front. (f) Tungsten probe (November 1990): Temporal profile of the temperature change rate observed via a 10 KΩ thermistor kept in front.

4.2. Comparison of calculations and measurements

Figure 6 shows ratio of the computed (C) to the measured (E) drop in the ^{92m}Nb activity rate across single probes. The largest departures, e.g. $C/E \sim 1.2$, are noted for Ti, Fe, SS304 and Cu. In principle, there are two sources of discrepancy: (i) discrepant transport and ^{93}Nb(n, 2n)^{92m}Nb cross-section data, (ii) unwar-

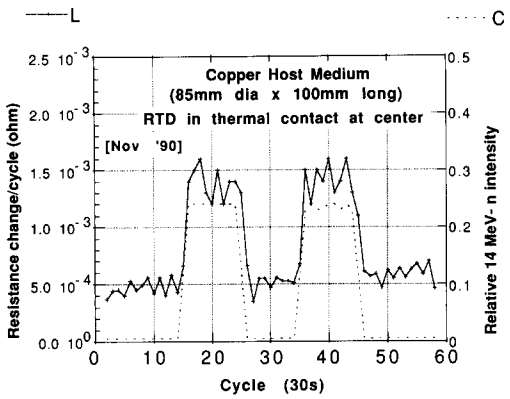

Fig. 4. Multiple probe host medium Copper (November 1990): Temporal profile of the temperature change rate observed via a 100 Ω platinum RTD kept in thermal contact at center.

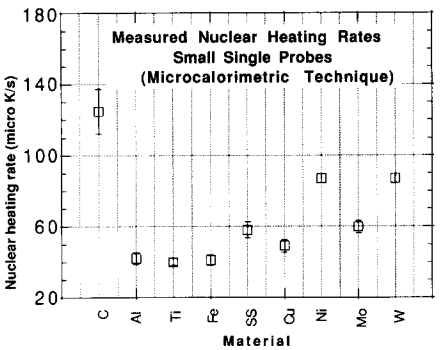

Fig. 5. Single probes: material-wise measured nuclear heating rate, expressed in units of μK/s for a normalizing source intensity of 10^{12} n/s; C, Ti, SS304, Ni, Mo and W data from the November 1990 experiments and those for Al, Fe and Cu from the December 1989 experiments.

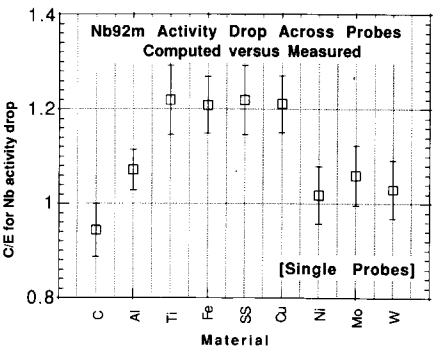

Fig. 6. Single probes: ratio of the computer (C) to the measured (E) drop in ^{92m}Nb activity across the probe, the activity drop is the ratio of the activity just behind a probe to that just ahead; C, T, SS304, Ni, Mo and W data from the November 1990 experiments and those for Al, Fe and Cu from the December 1989 experiments.

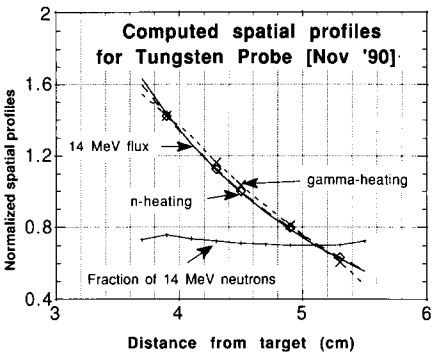

Fig. 7. Tungsten probe (November 1990): normalized spatial profiles of "14 MeV" flux, neutron heating rate, gamma heating rate, normalization is done with respect to each quantity averaged over the probe volume. Also provided is the spatial profile of fraction at "14 MeV" in the transmitted neutron flux.

ranted shift in the relative position of the probe inside the vacuum chamber during evacuation. Extreme sensitivity of the reaction rate drop can be gauged from fig. 7 that shows typical results of computations using MCNP for a single probe of W. Normalized spatial profiles of "14 MeV", flux, neutron heating rate and gamma heating rate are included. Normalization has been done with respect to the spatial average over the probe. This figure also provides a profile of the "14 MeV" fraction of the neutron flux. This fraction is practically constant. But, the other three quantities vary rapidly and are roughly driven by $1/d^2$ dependence, where d is the mean distance between the target and core of a probe. Before comparing the

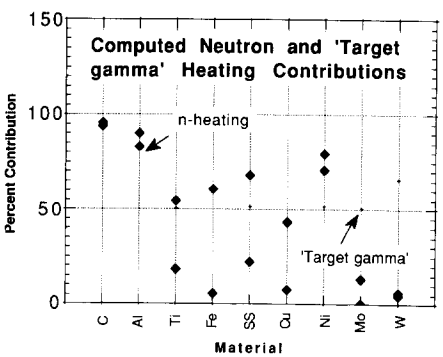

Fig. 8. Single probes: material-wise maximum and minimum percentual contributions of neutron heating alone to the computed heating rate. Also given is the percentual contribution of target γ's to the gamma (photon) heating rate of a probe.

measured and computed nuclear heating rates, it is useful to get a picture of the relative contributions of neutron and gamma heating, on one hand, and that of target γ's to the gamma heating rate evaluated for a probe. Figure 8 presents maximum and minimum percentual neutron heating contributions to the nuclear heating rate as a function of the materials. Usually, RMCCS yields the maximum contribution except for Mo and Cu; in fact, ENDL85 provides the maximum contribution as against the minimum by RMCCS for both Mo and Cu. KAOSLIB gives the minimum for C, Ti and SS304. Target γ's make dominating contributions of $\sim 92\%$ and 66% to the total gamma heating in C and W, respectively. However, their impact is larger on W where 95% of the total heating is due to γ's, unlike for C, where only 5% of total results from γ's.

For all single probes, there is a large spread in C/E's for a given probe material for different data libraries. This needs to be examined. In addition, the C/E's differ considerably from 1 for all materials as seen earlier [1]. C/E ranges for different materials are as follows: (1) graphite: 0.84–1.24, (2) aluminum: 1.03–1.81, (3) titanium: 0.42–1.00, (4) iron: 0.90–1.32, (5) stainless steel 304: 0.46–1.12, (6) copper: 0.79–1.28, (7) nickel: 0.89–1.26, (8) molybdenum: 0.77–0.89, (9) tungsten: 1.20–1.22. Mo and W provide the lowest spreads of all; however, the mean C/E is ~ 0.8 for Mo, while it is 1.2 for W.

For multiple probe systems, the experimental results for inserted host medium probes in iron and graphite have been compared to computed results obtained with the RMCCS library for heating numbers. Both measurements and computations show very little radial dependence. The experimental error is relatively large for copper probes. Hence they are not discussed. C/E for front probes is reasonable, e.g., 1.12 for iron and 1.05 for graphite. It is drastically lower, however, at mid-plane, being ~ 0.5 for iron and ~ 0.7 for graphite. Though experimental data for the spatial profile of the heat deposition in a copper medium suffers from large uncertainties, the averaged temperature change rate over the entire host medium has just 5% uncertainty. The C/E for this quantity is 0.89.

5. Conclusions

Direct nuclear heat deposition rate measurements, done using the microcalorimeteric technique in single probes of graphite, aluminum, titanium, iron, stainless steel 304, copper, nickel, molybdenum and tungsten, have demonstrated the feasibility of extracting this important data for fusion applications. Temperature change rates as low as 30 μK/s have been measured. Heat deposition rates as low as 35 μW/g have been measured. Thermistors and RTDs have generally provided matching experimental results. The point-sized bead thermistors used in the present experiments have opened up a whole range of possibilities for their extensive use to obtain nuclear heat deposition rates within thin material zones too. In fact, single probe experiments, done with iron without vacuum chamber, gave similar heat deposition rates as with vacuum chamber. Thus a vacuum chamber does not have to be an integral part of the measuring equipment. However, the drift goes up without vacuum chamber and it can make the task of extracting heat deposition rates subject to significant uncertainty in a weak radiation field.

Analysis of the measured data for single probes of all nine materials has revealed large discrepancies among various heating number/kerma factor evaluations themselves, on the one hand, and between measurements and the computations, on the other. Multiple probe systems too show discrepancies between the measurements and computations. These discrepancies have to be examined, both experimental data and computed data are to be looked at to find and understand the sources of discrepancy.

More experimentation is required to further improve the experimental accuracies obtained, on the one hand, and accumulate more data on various probe materials, on the other. This two-pronged approach will enable us to mitigate the concerns emanating from lack of testing of the computed kerma factors and related methodologies [3–11] and assumptions, apart from neutron and photon cross-section libraries for particle transport.

Acknowledgements

The United States Department of Energy, Office of Fusion Energy, via Grant no. DE-F603-86ER52124, and the Japan Atomic Energy Research Institute supported this effort.

References

[1] A. Kumar, Y. Ikeda and C. Konno, Experimental measurements and analysis of nuclear heat deposition rates in simulated D–T neutron environment: JAERI/USDOE Collaborative Program on Fusion Neutronics Experiments, Fusion Technol. 19 Parts 2A–2B (191) 1979–1988.

[2] A. Kumar, M.a. Abdou, Y. Ikeda and C. Konno, Radioactivity and nuclear heating measurements for fusion applications, 16th Symposium on Fusion Technology, 3–7 September, 1990, London, UK (Elsevier, Amsterdam, 1991), pp. 872–876.

[3] M.A. Abdou and C.W. Maynard, Calculation method for nuclear heating – part I: Theoretical and computational algorithms, Nucl. Sci. Engrg. 56 (1975) 360.

[4] M.A. Abdou and C.W. Maynard, Calculation methods for nuclear heating – part II: Applications to fusion-reactor blankets and shields, Nucl. Sci. Engrg. 56 (1975) 381.

[5] Y. Farawila, Y. Gohar and C. Maynard, KAOS-V Code: An evaluation tool for neutron kerma factors and other nuclear responses. Argonne National Laboratory report ANL/FPP/TM-240 (September 1989). Also by the same authors, KAOS/LIB-V: A library of nuclear response functions generated by KAOS-V code from ENDF/B-V and other data files, Argonne National Laboratory report ANL/FPP/TM-241 (april 1989).

[6] M.A. Abdou, C.W. Maynard and R.Q. Wright, MACK: A computer program to calculate neutron energy release parameters (fluence-to-kerma factors) and multigroup reaction cross sections from nuclear data in ENDF format, Oak Ridge National Laboratory report ORNL-TM-3994 (July 1973).

[7] R.E. Macfarlane, D.W. Muir and R.M. Boicourt, The NJOY nuclear data processing system, Volume II: The NJOY, RECONR, BROADR, HEATR, and THERMR Modules, Los Alamos National Laboratory report LA-9303-M, Vol. II (ENDF-324) (May 1982).

[8] R.S. Caswell and J.J. Coyne, Kerma factors for neutron energies below 30 MeV, Radiat. Res. 83 (1980) 217.

[9] R.J. Howerton, Calculated neutron kerma factors based on the LLNL ENDL data file, UCRL-50400 Vol. 27 (Jan. 1986).

[10] P.D. Soran and R.E. Seamon, Graphs of the cross sections in the recommended Monte Carlo cross-section library at the Los Alamos Scientific Laboratory, LA Report 8374-MS (May 1980).

[11] H.M. Fischer, A nuclear cross section data handbook, Los Alamos National Laboratory manual LA-11711-M (December 1989).

[12] S.R. Domen, Advances in calorimetry for radiation dosimetry, in: The Dosimetry of Ionizing Radiation, Vol. II, eds. K.R. Kase, B.E. Bjarngard and F.H. Attix, (Academic Press, Orlando, 1987) pp. 245–320.

[13] S.R. Gunn, Radiocalorimetric calorimetry: a review, Nucl. Instrum. Methods 29 (1964) 1; also two other later reviews with identical titles in Nucl. Instrum. Methods 85 (1970) 285 and Nucl. Instrum. Methods 135 (1976) 251.

[14] S.R. Domen and P.J. Lamperti, A heat-loss-compensated calorimeter: theory, design, and performance, J. Res. Natl. Bur. Stand. (USA) A 78 (5) (1974) 595.

[15] J.S. Laughlin and S. Genna, Calorimetry, in: Radiation Dosimetry, Vol. II, eds. F.H. Attix and W.C. Roesch (Academic Press, New York), pp. 380–441.

[16] J.C. Mcdonald, I-Chang Ma, B.J. Mijnheer and H. Zoetelief, Calorimetric and ionimetric dosimetry intercomparisons II; d+T neutron source at the Antoni van Leeuwenhoek Hospital, Med. Phys. 8 (1981) 1.

[17] Y.I. Aleksenko, G.V. Mukhima, L.P. Rokhlova and V.A. Khramchenkov, The use of Quasi-adiabatic calorimeters for interreactor dosimetry, At. Energ. 26 (1969) 328.

[18] A.W. Boyd and A. Keddar, Intercomparison of reactor calorimeters, At. Energy Rev. 8 (1970) 949.

[19] R.M. Carroll, R.B. Perez and O. Sisman, Measurements of nonfission heating in a high neutron flux reactor, Nucl. Sci. Engrg. 36 (1969) 232.

[20] F.H. Attix, Introduction to Radiological Physics and Radiation Dosimetry (Wiley, New York, 1986).

[21] J.F. Breismeister, ed. MCNP-A general Monte Carlo code for neutron and photon transport: version 3A, report no. LA-7396-M, Rev. 2 (Sep. 1988), along with MCNP3B newsletter dated July 18, 1988, Los Alamos National Laboratory.

[22] R.E. Seamon, a private communication (December 1990).

[23] R. Macfarlane, Energy balance of ENDF/B-V, Trans. Am. Nucl. Soc. 33 (1979) 681.

[24] R. Little and R. Seamon, Negative heating numbers, Los Alamos National Laboratory Memorandum to P. Young and E. Arthur, CSEWG Evaluations Committee (June 17, 1981).

[25] Y.S. Touloukian and E.H. Buyco, Specific heat: metallic elements and alloys, Vol. 4 of Series on Thermophysical Properties of Matter (IFI/Plenum, New York, 1970); see also, by same authors, "Specific heat: nonmetallic solids, Vol. 5 of the series, (IFI/Plenum, New York, 1970).